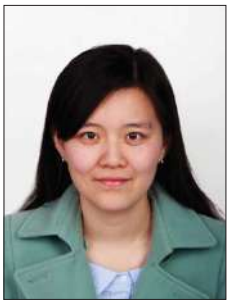

Yingxing Wang

Yuanyuan Li

Chunxiang Huang

DESIGN AND ANALYSIS OF DOUBLY SALIENT PERMANENT MAGNET DUAL-MECHANICAL PORT MOTOR FOR OFFSHORE SHIPS

DOI 10.15589/SMI20170111

Yingxing Wang Master of Engineering
Research direction: Design and control of permanent magnet motor
shadowwyx@sina.com

Yuanyuan Li Master of Engineering
Research direction: Mechanical structure design
82932625@qq.com

Chunxiang Huang Master of Engineering
Research direction: Mechanical and electrical equipment electrical control system design
ycgyhcx@126.com

Yancheng Vocational Institute of Industry Technology, Yancheng, 224000, China

Abstract. To meet the requirements of the energy power transmission of the hybrid propulsion system, this paper proposes a new type of the doubly salient permanent magnet dual-mechanical port motor. The structure, electromagnetic properties and temperature field analysis are investigated by means of the finite element analysis method. Besides, it studies the output characteristic by establishing a co-simulation model based on the field-circuit coupled method. The simulation results prove that the motor has inherited the advantages of the doubly salient permanent magnet motor, has high reliability and high power density. Meanwhile, the dual-mechanical port can realize the synthesis and distribution of the motor's energy flow under different operating conditions.

Keywords: doubly salient motor; finite element analysis; field-circuit coupled method; hybrid propulsion system.

References

[1] R.D. Geertsma, R.R. Negenborn, K. Visser, J.J. Hopman. Design and control of hybrid power and propulsion systems for smart ships: A review of developments [J]. Applied Energy, 2017, 194:.

[2] IMO. Third IMO greenhouse gas study 2014, executive summary and final report. Tech rep. London (UK): International Maritime Organisation (IMO); 2015.

[3] Volker T. Hybrid propulsion concepts on ships. In: Zeszyty Naukowe Akademii Morskiej w Gdyni, vol. 79; 2013. p. 66–76.

[4] Barcellos R. The hybrid propulsion system as an alternative for offshore vessels servicing and supporting remote oil field operations. In: Proceedings of the annual offshore technology conference, vol. 3; 2013. p. 16–31.

[5] K. T. Chau and C. C. Chan, Emerging energy-efficient technologies for hybrid electric vehicles [J]. Proceedings of the IEEE, 2007, 95(4): 821–835.

[6] E. Nordlund, P. Thelin, and C. Sadarangani, Four-quadrant energy transducer for hybrid electric vehicles [J]. Proc. 15th ICEM , Brugge, Belgium, 2004, 37–44

[7] Ping Zheng, Ranran Liu, P. Thelin, E. Nordlund, and C. Sadarangani, Research on the Cooling System of a 4QT Prototype Machine Used for HEV [J]. IEEE Transactions on energy conversion, 2008, 23(1): 61–67.

[8] Peter Pišek, Bojan Štumberger, Tine Marčič, etal. Design analysis and experimental validation of adouble rotor synchronous PM machine used for HEV [J], IEEE Transactions on Magnetics, 2013, 49(1): 152–155.

[9] J.T. Shi,Z.Q. Zhu,D. Wu,X. Liu. Comparative study of biased flux permanent magnet machines with doubly salient permanent magnet machines considering with influence of flux focusing[J]. Electric Power Systems Research,2016,:.

[10] Design, analysis and control of hybrid excited doubly salient stator-permanent-magnet motor[J]. Science China (Technological Sciences), 2010, 53(01):188-199.

[11] Pang Ting, Chen Xiao, Huang Shenghua, et al. ICE optimal efficiency control of electrical variable transmission [J].Transactions of China Electrotechnical Society, 2011, 25(6): 26–32 (in Chinese) .

[12] Wen Xuhui, Zhao Feng, Fan Tao, et al. Research on novel electrical variable transmission based on dual mechanical port electric machine [J]. Transactions of China Electrotechnical Society, 2007, 22(7): 24-28(in Chinese).

[13] W. Zhao, M. Cheng, W. Hua, et al. Back-EMF harmonic analysis and fault-tolerant control of flux-switching permanent-magnet machine with redundancy [J]. IEEE Transactions on Industrial Electronics, 2011, 52(5): 1546–1552.

Problem statement. With the improvement of environmental awareness and rapid development of marine tourism, the protection of coastal ecological environment is increasingly important [1]. Traditional diesel engine ships have poor emission reduction effects, while fully electric ships have a poor endurance. As a new type of ship propulsion system, hybrid propulsion power ship [2–4] has both advantages of the above two propulsion methods; it is even more economical, efficient and well controlled.

The hybrid propulsion system has two types of hybrid synthesis model. The mechanical type is relatively mature [5], and the electromagnetic type is more flexible, which can meet the dynamic matching requirements under different operating conditions. It has obvious advantages in the volume, power density and energy transmission efficiency [6].

At present, the research of electromagnetic hybrid synthesis mode and its dual-mechanical port motor mainly focuses on double rotor induction motor [7], permanent magnet synchronous motor [8], and switched reluctance motor. The double rotor induction motor and the switched reluctance motor have the advantages of low cost, high reliability and easy maintenance, but there are also problems of low efficiency and low power density. Meanwhile, the double rotor permanent magnet synchronous motor has a poor cooling performance due to the permanent magnets (PM) on the surfaces of the middle rotor.

In recent years, the doubly salient permanent magnet (DSPM) motor ([9–10]) has attracted the attention of many scholars because of its simple structure, high reliability and high power density. In this paper, based on the study of the single rotor DSPM motor, a new type of doubly salient permanent magnet dual-mechanical rotor is proposed for propulsion applications on offshore ships.

THE ARTICLE AIM is to introduce the structure and operating principle of the doubly salient permanent magnet dual-mechanical port motor, study its electromagnetic properties, temperature distribution and output characteristics by the finite element method, and then verify the feasibility of this structure.

Basic material

STRUCTURE AND PRINCIOLE

Structural parameter

The structure of the three-phase doubly salient permanent magnet dual-mechanical port motor is shown in Fig. 1. It is equivalent to two permanent magnet motors nested. The inner motor is a 12/8 pole DSPM motor, and the outer motor is a 24/16 pole DSPM motor; both share a middle rotor. The permanent magnets are embedded in the stator yoke and the inner rotor yoke. The inner and outer permanent magnetic fields pass through the middle rotor teeth respectively, and form a closed magnetic field by the middle rotor yoke.

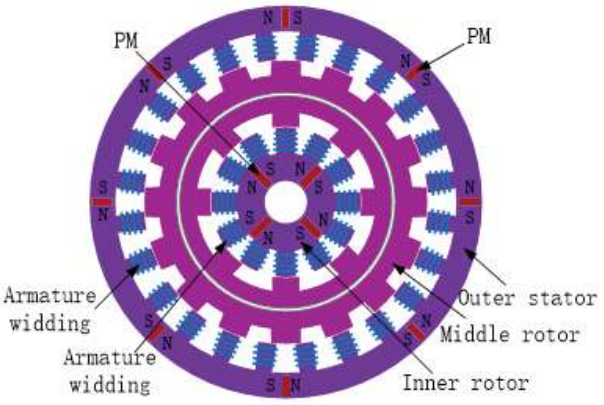

Fig. 1. Operation principle of dual-mechanical port hybrid power system

As supposed, the temperature rise of outer stator PMs can be easily managed. The inner rotor, which is directly connected to the output shaft of the engine, can be cooled by the cooling system of the engine. The middle rotor is a simple convex structure; it has a high mechanical strength, and also effectively avoids the problem of heat radiation.

To meet the requirement of offshore ship motor application, a 2 kW three-phase DSPM dual-mechanical port motor has been designed; both the inner and outer motors are 1 kW. According to the design principle of the doubly salient motor, the main design parameters of the motor are calculated, as shown in Table 1.

Operation principle

As shown in Fig. 2, the dual-mechanical port motor acts as the core component of the hybrid propulsion system. The inner rotor connects to the internal combustion engine (ICE), and the middle rotor is directly connected to the drive shaft. There is no mechanical connection

Table 1. Main dimensions of the motor

Stator outer diameter /mm	286
Stator inner diameter /mm	221
Stator yoke height /mm	21.5
Stator tooth width /°	7.5
Middle motor inner diameter /mm	100
Middle rotor outer diameter /mm	208
Middle rotor yoke height /mm	30
Middle rotor tooth width /°	10.8/20
Shaft length /mm	75
Shaft diameter /mm	30
Inner rotor outer diameter /mm	99
Inner rotor yoke height /mm	20
Inner rotor tooth width /mm	15°
Permanent magnet size /mm	6×18
Stator winding /turns	280
Inner rotor winding /turns	200
Air gap /mm	0.5

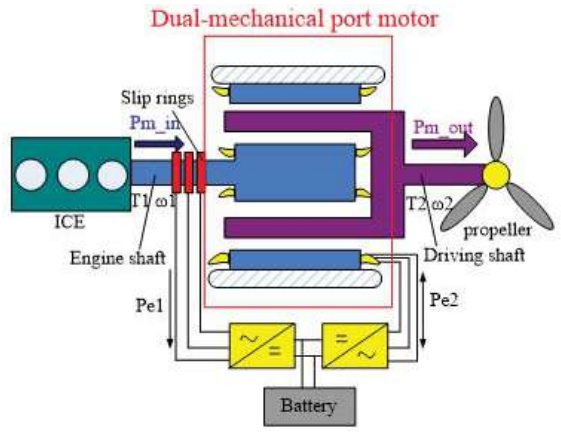

Fig. 2. Operation principle of dual-mechanical port hybrid power system

between the ICE and the drive shaft, which keeps the ICE operating in the best fuel economy zone [11]. Two sets of inverters are needed in this system, one for stator windings and the other for the inner rotor windings; for simplicity, they share the same battery.

The environment of the offshore navigation is complex and changeable. In order to meet the requirements of different operating conditions, we need to control the inner and outer motors operation in different states to achieve the synthesis and distribution of the energy flow [12].

When the ship is employed for fishing at a low speed, the outer motor works in the pure electric mode, and the propeller is driven by the middle rotor. At that, the battery is the only energy source.

When the ship sails at a high speed, the ICE provides energy and drives the inner rotor to transfer energy to outer motor through the electromagnetic field. Since the ICE always works in the best fuel economy zone; its torque and speed do not coincide with the actual demand of the current navigation. At that, the energy must be adjusted between the inner motor, the outer motor, and the energy storage device. When the ship accelerates and overloads, the energy demand is high, and both the ICE and the battery provide energy.

During deceleration or braking, both the inner motor and the outer motor work in the generation mode, and the surplus energy can be fed back to the storage battery to reduce the battery loss.

FINITE ELEMENT ANALYSIS

Magnetic field distribution

Fig. 3 shows the magnetic field distribution in the unloaded state. It can be seen that an air circle is added to the outside of the motor as a boundary condition, because the stator permanent magnet motor has an external magnetic leakage. As shown in Fig. 3, *a*, flux lines of the inner and outer motors form a closed magnetic circuit through the middle rotor, following the "minimum

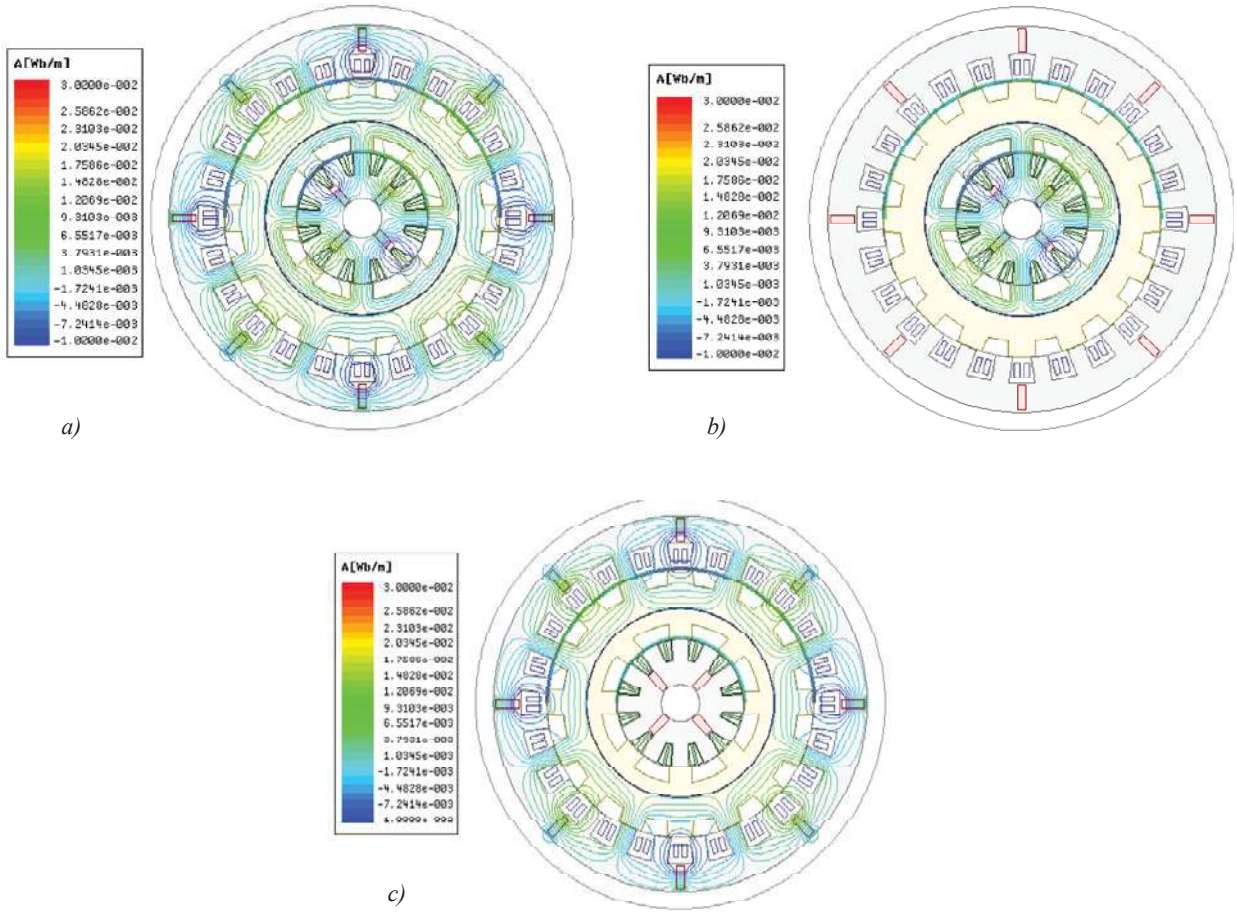

Fig. 3. Magnetic field distributions in unloaded state: *a* — both the PMs of inner and outer motor affected; *b* — only the PMs of inner motor affected; *c* — only the PMs of outer motor affected

magnetic reluctance principle". In order to analyze the magnetic field coupling of the inner and outer motors, Fig. 3, *b* and *c* show the no-load magnetic field affecting separately the PMs of the inner and outer motors. The magnetic field coupling between the inner and outer motors is minimal. Therefore, this paper analyzes the static characteristics of the inner and outer motors, such as magnetic linkage, back EMF, etc., and studies its output performance by means of the field-circuit coupled transient co-simulation.

Fig. 4 shows the flux density waveform of the air gap for both the inner and outer motors. It can be seen that the maximum value of the flux density remains constant at the overlapping region between the stator and rotor's air gap, which is related to stator and rotor pole arc. Taking into account that the flux density amplitude in the air gap can directly reflect the magnetic field intensity of the motor, the mentioned amplitudes of the inner and outer motors should be set reasonably.

Flux Linkage and Back EMF

Fig. 5 shows the relationship between the permanent magnet flux and the rotor position angle of the internal and external motor at rated speed. The maximum value appears in the overlapping region between the stator and rotor teeth. When the motor is operating, it can make sure that the phase current can be commutated correctly.

Furthermore, according to the characteristics of the flux linkage, the no-load back EMF can be deduced as follows:

$$e = \frac{d\psi_{pm}}{dt} = N\frac{d\varphi_{pm}}{d\theta}\omega_r . \qquad (2)$$

Formula (2) shows us that the back EMF is proportional to the winding turns N and the motor angular velocity ω_r, so that the change of back EMF reflects the variation of the magnetic field.

As shown in Fig. 6, the no-load EMF waveform at the rated speed nearly retains the shape of a square wave, which is similar to the brushless DC motor. However, the harmonic component of the back EMF is larger than an ideal square wave due to the influence of the magnetic leakage and slowly changing flux linkage in the overlapping region between stator and rotor teeth. Therefore, the traditional square wave control or sinusoidal wave control can be used when formulating control strategies.

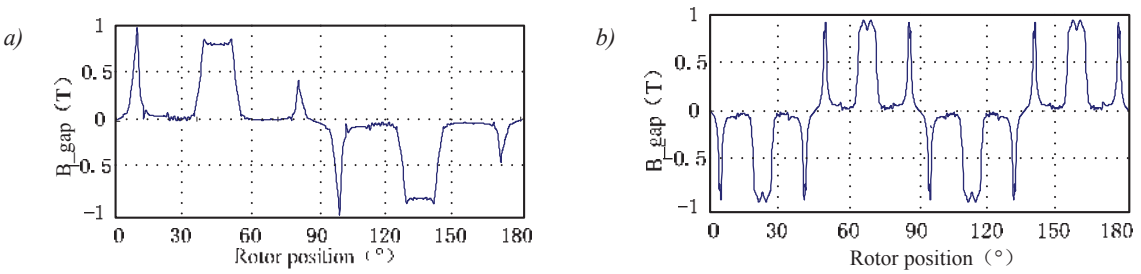

Fig. 4. Flux density distributions: *a* — in the inner motor's air gap; *b* — in the outer motor's air gap

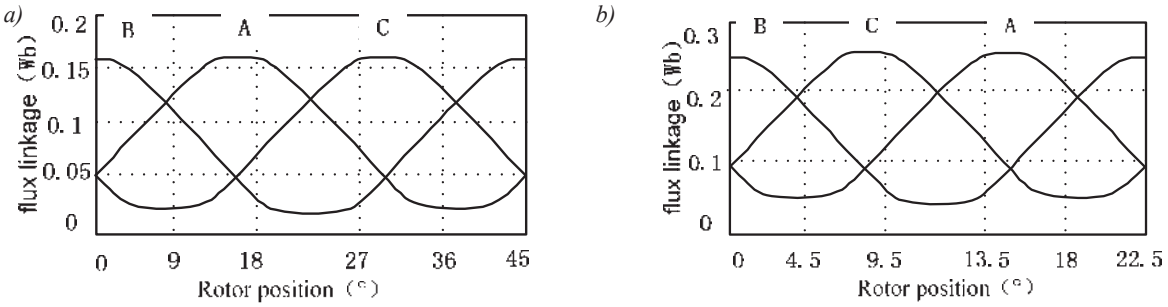

Fig. 5. Permanent magnet flux linkage in no-load condition: *a* — of the inner motor at the rated speed; *b* — of the outer motor at the rated speed

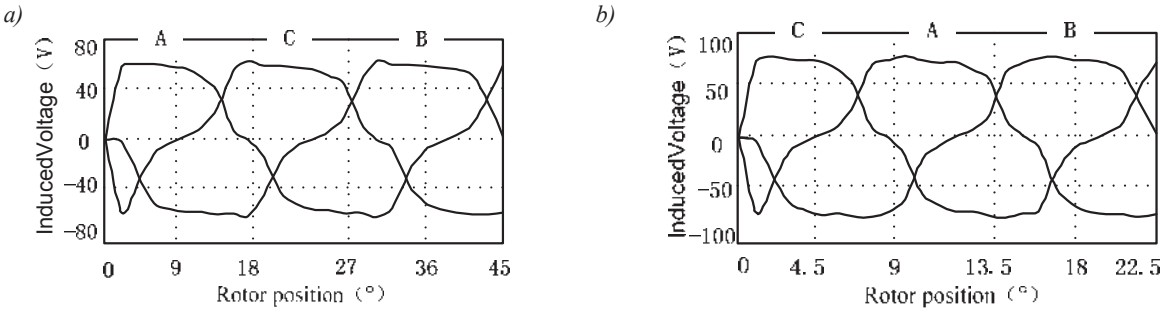

Fig. 6. Back EMF in no-load condition: *a* — of the inner motor at the rated speed; *b* — of the inner motor at the rated speed

Inductance

The inductance characteristic of the permanent magnet motor affects the torque and power of motor directly. Let us consider the A phase as an example.

When the current of the A phase is energized independently, the total flux of the winding is

$$\psi = L_a i_a + \psi_{pm}, \quad (3)$$

where ψ is the flux linkage, ψ_{pm} is the magnetic flux linkage, i_a is winding phase current.

Fig. 7 shows that the permanent magnetic field is the main magnetic field of the motor when the armature current is 0 A, while the armature current regulates the magnetic field strength to a certain extent. When the armature current varies from –8 A to 8 A, the winding flux increases accordingly. It is obvious that the positive current has an increased magnetic effect on the permanent magnetic field; however, the negative current has a weak magnetic effect on the permanent magnetic field. In addition, the greater the amplitude of the current is, the greater the impact on the main magnetic field is.

The inductance of the A phase winding can be calculated as follows:

$$L_a = \frac{\psi - \psi_{pm}}{i_a}. \quad (4)$$

Fig. 8 shows the self-inductance curves of the inner and outer motors under different armature currents. Obviously, the inductance is related not only to the rotor position, but also to the armature current. It can be clearly seen that the armature magnetic field can regulate the permanent magnetic field of inner motor. The inductance of the winding is lower when the magnetic flux increases, and higher when the magnetic flux is weak. However, the self-inductance of the outer motor is not obvious because of the low saturation magnetic field.

Fig. 9 shows the mutual inductance between the inner and outer motors under different armature current. It can be seen that the mutual inductance amplitude is much smaller than its self-inductance. It is further verified that coupling of the armature magnetic field between the inner and outer motors is very small.

Temperature field distribution

Considering the special environment of this marine permanent magnet motor application, it is necessary to ensure that its temperature rise will not affect the reliability and stability of the motor. The maximum temperature of the motor is observed under acceleration and heavy load. At that, the two sets of armature windings produce copper consumption, which becomes the main heat source of the motor. In this section, we analyze the steady-state temperature field of the motor by establishing a joint simulation model with Ansoft14.0 and ANSYS Workbench.

The high temperature will cause irreversible demagnetization of permanent magnetic material, which will lead to the malfunction of the ship. In order to avoid this situation, let us adopt two tapes of the cooling-down method, including natural water cooling and air cooling. Firstly, a waterway is added to the stator housing and led to the inner rotor; then, it flows through the motor shaft. At last, it constitutes a cycle through the internal-combustion engine.

Fig. 10 shows the heat flux distribution of the motor. The heat flux value of the middle rotor is small because it employs natural air cooling. The motor shell and the rotating shaft make use of natural water cooling, and its heat dissipation coefficient is higher.

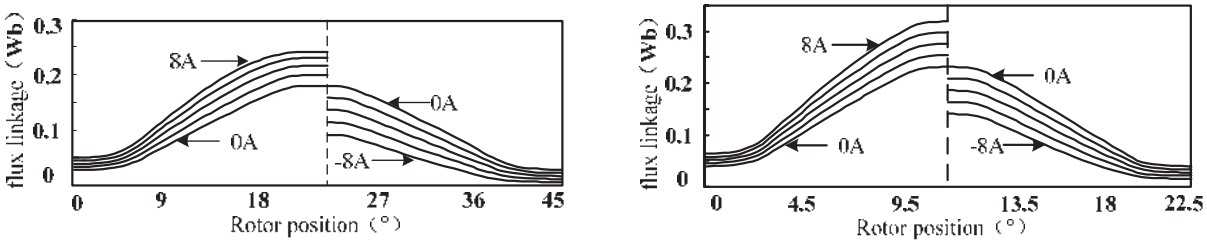

Fig. 7. Flux linkage under different armature current: *a* — of the inner motor; *b* — of the outer motor

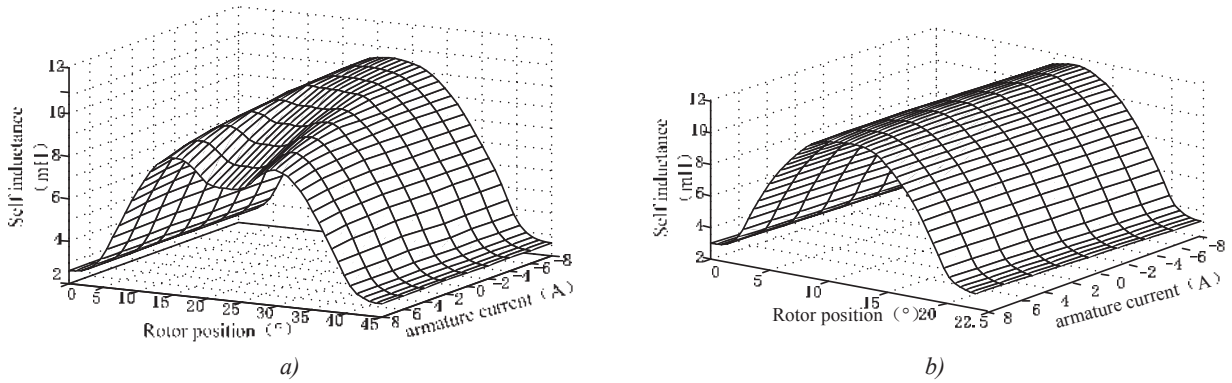

Fig. 8. Self-inductance of armature winding under different armature current: *a* — of the inner motor; *b* — of the outer motor

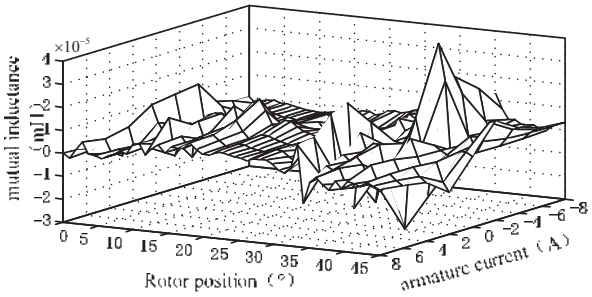

Fig. 9. Mutual inductance of armature winding under different armature current

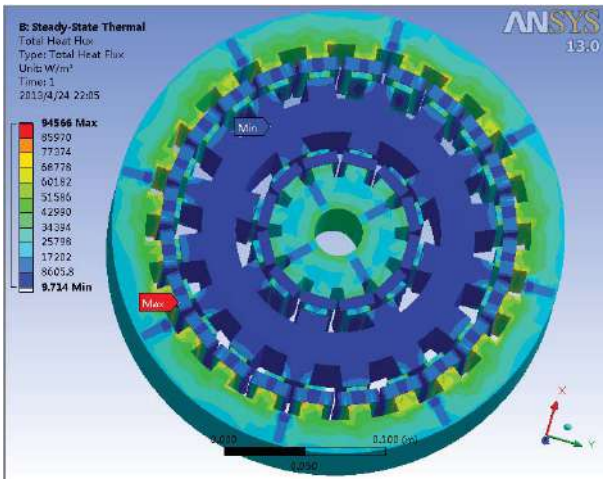

Fig. 10. Heat flux distribution

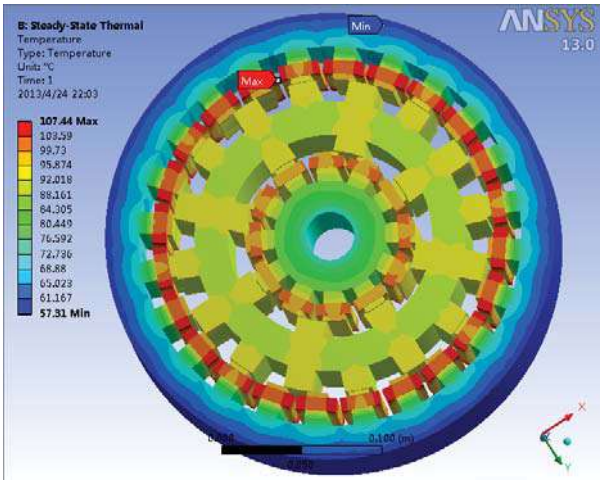

Fig. 11. Temperature distribution

It is assumed that the ambient temperature is 40 °C. Fig. 11 shows the temperature distribution inside the motor. The temperature of the stator casing and the inner rotor is lower, and the temperature of the permanent magnet in the inner rotor and the outer stator is respectively about 80°C and 65 °C, which is lower than the maximum operating temperature of the permanent magnet. Besides, the maximum temperature is observed in the stator armature winding, which is 107.44 °C, and the temperature rise is acceptable. It is obvious that the cooling system can take most of the motor heat.

Output Torque

Considering the coupling between the electric and magnetic circuit, this paper adopts the "field-circuit coupled transient co-simulation" method. Compared with the traditional mathematical modeling method, this method can effectively improve the simulation accuracy, and thus realize the overall performance simulation of the new doubly salient permanent magnet dual-mechanical port motor by studying the torque characteristics.

As shown in Fig. 12, the drive circuit employs a full bridge power converter, sets the peak value of the reference input current to 8 A, and uses sine wave control to analyze the steady-state operation characteristics.

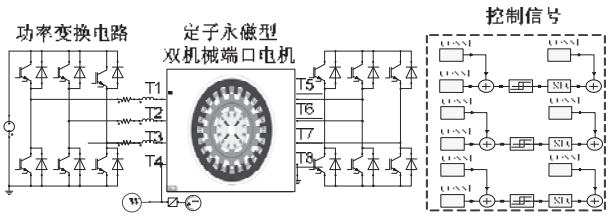

Fig. 12. Control system model under sinusoidal control

Fig. 13 shows the output torque waveforms of the motor under different operating conditions. Both the inner and outer motors have good mechanical properties, which will meet the power demand of the hybrid power system under several operational conditions. Also, there is a clear motor torque ripple, mainly due to the doubly salient structure of the motor. and the torque ripple. It can be reduced with the help of the precise control method [13].

Table 2 compares the output torque characteristics under three different operating conditions. It can be seen that the theoretical value of the motor output torque is basically consistent with the simulation results, which shows that the design of the prototype is correct and reasonable.

Table 2. Torque characteristics under different conditions

	T_{ave} /(N·m)	T_{ave} /(N·m)	K_T/(%)
only inner motor	10.523	9.55	33.665
only outer motor	20.1856	19.1	29.738
both inner and outer motor	31.0584	28.65	40.599

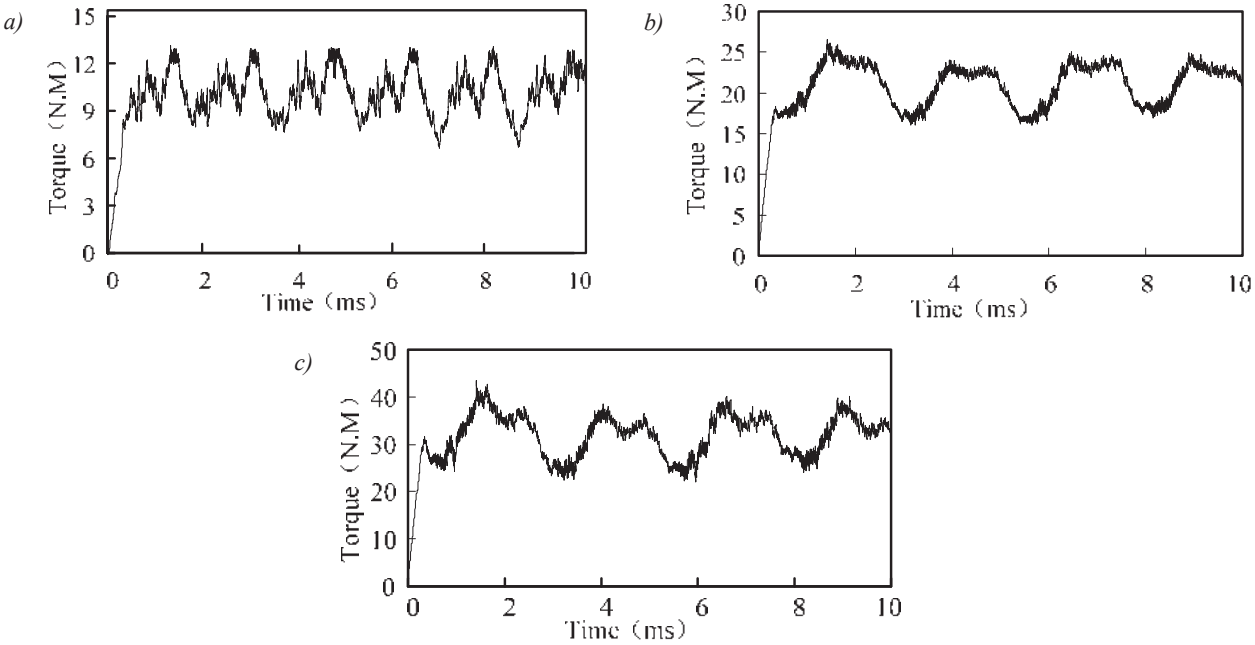

Fig. 13. The output torque at the rated speed: *a* — for the inner motor; *b* — for the output motor; *c* — total output of the inner and the outer motors

CONCLUSION. This paper presents a doubly salient permanent magnet dual-mechanical ports motor used in the hybrid propulsion system of an offshore ship. Its operating principle and the finite element analysis results are given in detail. The simulation results show that the motor inherits the merits of both the dual-mechanical port motor and the DSPM motor. In addition, the temperature field analysis and the torque characteristics also show that the proposed motor can meet the torque demand of the hybrid propulsion system under different operational conditions.

Статью рекомендует в печать
д-р техн. наук, проф. *Г. В. Павлов*